Cooperative electromagnetic interactions between nanoparticles for solar energy harvesting

Mathieu Langlais, Jean-Paul Hugonin, Mondher Besbes, Philippe Ben-Abdallah

Cooperative electromagnetic interactions between nanoparticles for solar energy harvesting

Mathieu Langlais,[1,2] **Jean-Paul Hugonin,**[2] **Mondher Besbes**[2] **and Philippe Ben-Abdallah**[2,*]

[1]*Total New Energies, R&D, Tour Michelet, 92078 Paris La Défense Cedex, France*
[2]*Laboratoire Charles Fabry,UMR 8501, Institut d'Optique, CNRS, Université Paris-Sud 11, 2, Avenue Augustin Fresnel, 91127 Palaiseau Cedex, France*

[*] *pba@institutoptique.fr*

Abstract: The cooperative electromagnetic interactions between discrete resonators have been widely used to modify the optical properties of metamaterials. Here we propose a general approach for engineering these interactions both in the dipolar approximation and for any higher-order description. Finally we apply this strategy to design broadband absorbers in the visible range from simple n-ary arrays of metallic nanoparticles.

References and links

1. H. A. Atwater and A. Polman, "Plasmonics for improved photovoltaic devices," Nat. Mater. **9**, 205–2013 (2010).
2. 10. P. Bermel, M. Ghebrebrhan, W. Chan, Y. X. Yeng, M. Araghchini, R. Hamam, C. H. Marton, K. F. Jensen, M. Soljacic, J. D. Joannopoulos, S. G. Johnson, and I. Celanovic, "Design and global optimization of high-efficiency thermophotovoltaic systems," Opt. Express **18**, A314–A334 (2010).
3. A. Ashkin, J. M. Dziedzic, J. E. Bjorkholm, and S. Chu, "Observation of a single-beam gradient force optical trap for dielectric particles," Opt. Lett. **11**, 288–290 (1986).
4. A. N. Poddubny, P. A. Belov, and Y. S. Kivshar, "Spontaneous radiation of a finite-size dipole in hyperbolic media," Phys. Rev. A **84**, 023807 (2011).
5. N. I. Landy, S. Sajuyigbe, J. J. Mock, D. R. Smith and W. J. Padilla, "Perfect metamaterial absorber," Phys. Rev. Lett. **100**, 207402 (2008).
6. K. Aydin, V. E. Ferry, R. M. Briggs and H. A. Atwater, "Broadband polarization-independent resonant light absorption using ultrathin plasmonic super absorbers," Nat. Commun. **2**, 517 (2011).
7. S. D. Jenkins and J. Ruostekoski, "Metamaterial transparency induced by cooperative electromagnetic interactions," Phys. Rev. Lett. **111**, 147401 (2013).
8. V. A. Fedotov, N. Papasimakis, E. Plum, A. Bitzer M. Walther, P. Kuo, D. P. Tsai and N. I. Zheludev, "Spectral collapse in ensembles of metamolecules," Phys. Rev. Lett. **104**, 223901 (2010).
9. P. Ben-Abdallah, R. Messina, S.-A. Biehs, M. Tschikin, K. Joulain, and C. Henkel, "Heat superdiffusion in plasmonic nanostructure networks," Phys. Rev. Lett. **111**, 174301 (2013).
10. R. Messina, M. Tschikin, S.-A. Biehs, and P. Ben-Abdallah, "Fluctuation-electrodynamic theory and dynamics of heat transfer in systems of multiple dipoles," Phys. Rev. B **88**, 104307 (2013).
11. E. M. Purcell and C. R. Pennypacker, "Scattering and absorption of light by nonspherical dielectric grains," Astrophys. J. **186**, 705 (1973).
12. B. T. Draine and P. J. Flateau, "Discrete-dipole approximation for periodic targets: theory and tests," J. Opt. Soc. Am. A. **25**, 2693 (2008).
13. A. B. Evlyukhin, C. Reinhardt, A. Seidel, B. S. Luk'yanchuk, and B. N. Chichkov, "Optical response features of Si-nanoparticle arrays," Phys. Rev. B **82**, 045404 (2010).
14. M. S. Tomas, "Green function for multilayers: light scattering in planar cavities," Phys. Rev. A **51**, 2545 (1995).

15. P. P. Ewald, "Die berechnung optischer und elektrostatischer gitterpotentiale," Annalen der Physik, **369**, 253–287 (1921).
16. F. Capolino, D. Wilton, and W. Johnson, "Efficient computation of the 2-D Green's function for 1-D periodic structures using the Ewald method," IEEE Trans. on Antennas and Propaga. **53**, 9 (2005).
17. E. Castanie, R. Vincent, R. Pierrat, and R. Carminati, "Absorption by an optical dipole antenna in a structured environment," Int. J. Opt. **2012**, 452047 (2012).
18. P. Ben-Abdallah, S.-A. Biehs, and K. Joulain, "Many-body radiative heat transfer theory," Phys. Rev. Lett. **107**, 114301 (2011).
19. J. D. Jackson, *Classical Electrodynamics*, 3rd ed. (John Wiley, 1999).
20. C. F. Bohren, D. R. Huffman, Absorption and Scattering of Light by Small Particles (Wiley Science, New York, 1998).
21. A. B. Evlyukhin, C. Reinhardt, U. Zywietz, and B. N. Chichkov, "Collective resonances in metal nanoparticle arrays with dipole-quadrupole interactions," Phys. Rev. B **85**, 245411, (2012).
22. L. Schwartz, Théorie des distributions, Hermann (1951).
23. B. Stout, J.-C. Auger and J. Lafait, "A transfer matrix approach to local field calculations in multiple scattering problems," J. Mod. Opt. **49**, 2129–2152 (2002).
24. E. D. Palik, *Handbook of Optical Constants of Solids* (Academic Press, New York, 1998).
25. E. E. Narimanov, A. V. Kildishev, "Optical black hole: broadband omnidirectional ligh absorber," Appl. Phys. Lett. **95**, 041106 (2009).
26. A. Aubry, D. Y. Lei , A. I. Fernández-Domínguez , Y. Sonnefraud , S. A. Maier, and J. B. Pendry, "Plasmonic light-harvesting devices over the whole visible spectrum," Nano. Lett. **10**, 2574–2579 (2010).
27. N. P. Sergeant, O. Pincon, M. Agrawal, and P. Peumans, "Design of wide-angle solar selective absorbers using aperiodic metal-dielectric stacks," Opt. Express **17**, 22800–22812 (2009).
28. J. H. Holland, *Adaptation in Natural and Artificial Systems* (MIT Press/Bradford Books Edition, Cambridge, MA, 1992).
29. T. Feichtner, O. Selig, M. Kiunke, and B. Hecht, "Evolutionary optimization of optical antennas," Phys. Rev. Lett. **109**, 127701 (2012).
30. J. Drevillon and P. Ben-Abdallah, "Ab initio design of coherent thermal sources," J. Appl. Phys. **102**, 114305 (2007).
31. L. Landau, E. Lifchitz, and L. Pitaevskii, *Electromagnetics of Continuous Media* (Pergamon, Oxford, 1984).

1. Introduction

Engineering light-matter interactions is a longstanding problem in physics and is of prime importance for numerous technological applications such as the photo and thermophovoltaic energy conversion [1, 2], the optical manipulation of nanoobjects [3] or the quantum information treatment [4]. Light interaction with resonant structures embedded inside a material is a natural way to modify its optical properties. To date, a large number of resonant structures have been developped following such a strategy. Among these, metamaterials based on metallo-dielectric structures have been proposed to operate at frequencies ranging from the microwave domain [5] to the visible [6].

The design of artificially constructed magnetodielectric resonators which strongly interact cooperatively is a very recent and promising way to generate metamaterials that highlight innovative physical [7, 8] and transport [9, 10] properties. However, so far, only heuristic approaches have been followed to identify the convenient meta-structures which display target functionalities. In this paper, we present a general theory to describe the multiple scattering interactions mechanisms in discret networks of resonators embedded in a host material and we propose a general method to identify the appropriate inner structure of networks that highlight a targeted optical property either by considering the interacting objects as simple (electric and magnetic) dipoles or as multipoles of arbitrary order. To illustrate the strong potential of cooperative interactions to tailor the optical properties of materials we design a broadband light absorber made with simple binary lattices of metallic nanoparticles immersed in a transparent host material.

2. Scattering by nanoparticle networks in the dipolar approximation

To start, let us consider a set of objects dispersed inside a host material as depicted in Fig. 1. Suppose this system is higlighted by an external harmonic electromagnetic field of wavelength much larger than the typical size of objects. In this condition, we can associate to each object an electric (E) and magnetic (H) dipole moment $\mathbf{p}_{m;A}(A=E,H)$ (the higher orders contributions are discussed in the next paragraph). The local electromagnetic field $\mathbf{A}^{ext}(\mathbf{r}_m)$ at the dipoles location $\mathbf{r}_m$ results from the superposition of external incident field, the field generated by the others dipoles and the auto-induced field which comes from the interactions with the interfaces. Therefore it takes the form [11, 12, 13]

$$\mathbf{A}_m^{ext} = \mathbf{A}_m^{inc} - i\omega \sum_{B=E,H} \Gamma_{AB}(\Delta\mathbb{G}_{mm}^{AB}\mathbf{p}_{m;B} + \sum_{n\neq m} \mathbb{G}_{mn}^{AB}\mathbf{p}_{n;B}), \tag{1}$$

where $\begin{pmatrix} \Gamma_{EE} & \Gamma_{EH} \\ \Gamma_{HE} & \Gamma_{HH} \end{pmatrix} \equiv \begin{pmatrix} i\omega\mu_0 & \omega/c \\ \omega/c & -i\omega\varepsilon_0 \end{pmatrix}$ and $\mathbb{G}_{mn}^{AB}$ is the dyadic Green tensor in the host material which takes into account the presence of interfaces [14] and gives the field $\mathbf{A}$ at the position $\mathbf{r}_m$ given a $\mathbf{B}$-dipole located in $\mathbf{r}_n$. $\Delta\mathbb{G}^{AB}$ defined as $\Delta\mathbb{G}^{AB} \equiv \mathbb{G}^{AB} - \mathbb{G}_0^{AB}$ gives the contribution of interfaces only.

Here $\mathbb{G}_0^{AB}(\mathbf{r}_m,\mathbf{r}_n) = \frac{\exp(ikr_{mn})}{4\pi r_{mn}} \times \begin{cases} \left[\left(1+\frac{ikr_{mn}-1}{k^2r_{mn}^2}\right)\mathbb{1} + \frac{3-3ikr_{mn}-k^2r_{mn}^2}{k^2r_{mn}^2}\widehat{\mathbf{r}}_{mn}\otimes\widehat{\mathbf{r}}_{mn}\right] & if A=B \\ \frac{ikr_{mn}-1}{kr_{mn}}\mathbb{L} & if A\neq B \end{cases}$ is the free space Green tensor in the host material defined with the unit vector $\widehat{\mathbf{r}}_{mn} \equiv \mathbf{r}_{mn}/r_{mn}$. $\mathbf{r}_{mn}$ denotes here the vector linking the center of dipoles m and n, while $r_{ij} = \mid \mathbf{r}_{ij} \mid$, k is the wavector, $\mathbb{1}$ the unit dyadic tensor and $\mathbb{L} = \begin{pmatrix} 0 & -\hat{r}_{mn,z} & \hat{r}_{mn,y} \\ \hat{r}_{mn,z} & 0 & -\hat{r}_{mn,x} \\ -\hat{r}_{mn,y} & \hat{r}_{mn,x} & 0 \end{pmatrix}$. Beside the dipoles location the auto-induced part of field does not exist anymore and it takes the simplified form

$$\mathbf{A}^{ext}(\mathbf{r}) = \mathbf{A}^{inc}(\mathbf{r}) - i\omega \sum_{B=E,H} \Gamma_{AB} \sum_j \mathbb{G}^{AB}(\mathbf{r}-\mathbf{r}_j)\mathbf{p}_{j;B}. \tag{2}$$

It immediately follows that, the dipolar moments associated to each object reads

$$\mathbf{p}_{m;A} = \chi_A \overleftrightarrow{\alpha}_{m;A} \mathbf{A}_m^{ext} \tag{3}$$

where χ_A represents either the vacuum permittivity ε_0 or the vacuum permeability μ_0 and $\overleftrightarrow{\alpha}_{i,A}$ is the free polarizability tensor of m^{th} object under the action of field $\mathbf{A}$. By inserting the external contribution (1) of local field into relation (23) we get the following system which relates all dipole moments

$$\mathbf{p}_{m;A} = \chi_A \overleftrightarrow{\alpha}_{m;A}[\mathbf{A}_m^{inc} - i\omega \sum_n \sum_{B=E,H} \mathbb{G}_{reg}^{AB}(r_m,r_n)\mathbf{p}_{n;B}]. \tag{4}$$

Here, where we have introduced the regularized Green tensor

$$\mathbb{G}_{reg}^{AB}(r,r') = \begin{cases} \Gamma_{AB}\mathbb{G}^{AB}(r,r') \; if \; r\neq r' \\ \Gamma_{AB}\Delta\mathbb{G}^{AB}(r,r') \; if \; r=r' \end{cases}. \tag{5}$$

In the particular case of n-ary periodic lattices made with n arbitrary dipoles of free electric and magnetic polarizability $\overleftrightarrow{\alpha}_{m;A=E,H}$ distributed in a unit cell we have, according to the periodicity, the supplementary relations for the incident fields $\mathbf{A}_{j_\beta}^{inc} = \widetilde{\mathbf{A}_\beta} exp(i\mathbf{k}_{//}.\mathbf{r}_{j_\beta})$ and for the dipolar moments $\mathbf{p}_{j_\beta;A} = \widetilde{\mathbf{p}}_{\beta;A} exp(i\mathbf{k}_{//}.\mathbf{r}_{j_\beta})$. Here $\mathbf{r}_{j_\beta}$ is the position vector of the β^{th} dipole inside the unit cell j of lattice and $\mathbf{k}_{//}$ is the parallel component of wavector.

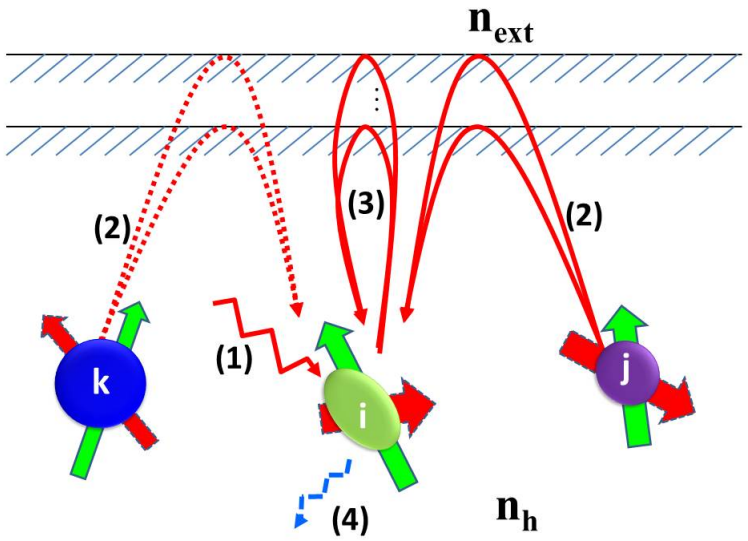

Fig. 1. Multiple light scattering interactions in a set of subwavelength plasmonic structures embeded in a transparent host material of refractive index n_h. In the dipolar approximation each object is replaced by both a dipolar electric moment and a magnetic moment. The external field felt by each object decomposes into (1) the incident field, (2) the field radiated by the other objects and (3) the auto-induced field which comes from the interface after being emitted by the object itself. All dipoles radiate (4) in their surrounding.

Accordingly, Eq. (4) can be solve with respect to the incident field to give

$$\begin{pmatrix} \widetilde{\mathbf{p}}_E \\ \widetilde{\mathbf{p}}_H \end{pmatrix} = \mathscr{A}^{-1}\mathscr{H}\begin{pmatrix} \widetilde{\mathbf{E}} \\ \widetilde{\mathbf{H}} \end{pmatrix}. \tag{6}$$

Here we have set $\widetilde{\mathbf{p}}_{A=E,H} = \begin{pmatrix} \widetilde{\mathbf{p}}_{1,A}, & \cdots, & \widetilde{\mathbf{p}}_{n,A} \end{pmatrix}^t$ and $\widetilde{\mathbf{A}} = \begin{pmatrix} \widetilde{\mathbf{A}}_1, & \cdots, & \widetilde{\mathbf{A}}_n \end{pmatrix}^t$ and we have define the block matrixes

$$\mathscr{H} = diag(\varepsilon_0 \overleftrightarrow{\alpha}_{1;E}, \ldots, \varepsilon_0 \overleftrightarrow{\alpha}_{n;E}, \mu_0 \overleftrightarrow{\alpha}_{1;H}, \ldots, \mu_0 \overleftrightarrow{\alpha}_{n;H}) \tag{7}$$

and

$$\mathscr{A} = \begin{pmatrix} (\mathbb{1}+\mathbb{U}_{11}^{EE}) & \mathbb{U}_{12}^{EE} & \cdots & \mathbb{U}_{1n}^{EE} & \mathbb{U}_{11}^{EH} & \cdots & \mathbb{U}_{1n}^{EH} \\ \mathbb{U}_{21}^{EE} & \ddots & & \vdots & \vdots & & \vdots \\ \vdots & \ddots & (\mathbb{1}+\mathbb{U}_{nn}^{EE}) & \mathbb{U}_{n-1,n}^{EE} & \mathbb{U}_{n1}^{EH} & \cdots & \mathbb{U}_{nn}^{EH} \\ \mathbb{U}_{n1}^{EE} & \cdots & \mathbb{U}_{n,n-1}^{EE} & (\mathbb{1}+\mathbb{V}_{11}^{HH}) & \mathbb{V}_{12}^{HH} & \cdots & \mathbb{V}_{1n}^{HH} \\ \mathbb{V}_{11}^{HE} & \cdots & \mathbb{V}_{1n}^{HE} & \mathbb{V}_{21}^{HH} & \ddots & \ddots & \vdots \\ \vdots & & \vdots & \vdots & \ddots & \ddots & \mathbb{V}_{n-1,n}^{HH} \\ \mathbb{V}_{n1}^{HE} & \cdots & \mathbb{V}_{nn}^{HE} & \mathbb{V}_{n1}^{HH} & \cdots & \mathbb{V}_{n,n-1}^{HH} & (\mathbb{1}+\mathbb{V}_{nn}^{HH}) \end{pmatrix} \tag{8}$$

with

$$\mathbb{U}_{lk}^{EA} = i\varepsilon_0\omega \overleftrightarrow{\alpha}_{l;E} \sum_j \mathbb{G}_{reg}^{EA}(\mathbf{r}_{0l}, \mathbf{r}_{jk}) e^{i\mathbf{k}_{//}\cdot(\mathbf{r}_{jk}-\mathbf{r}_{0l})}, \tag{9}$$

$$\mathbb{V}_{lk}^{HA} = i\mu_0\omega\overleftrightarrow{\alpha}_{l;H}\sum_j \mathbb{G}_{reg}^{HA}(\mathbf{r}_{0l},\mathbf{r}_{jk})e^{i\mathbf{k}_{//}.(\mathbf{r}_{jk}-\mathbf{r}_{0l})}. \tag{10}$$

These summations can calculated directly or using the Ewald's method [15, 16] as in solid-state physics. Relation (6) defines the dressed polarizability tensor [17]

$$\Lambda \equiv \mathscr{A}^{-1}\mathscr{H} = \begin{pmatrix} \Lambda^{EE} & \Lambda^{EH} \\ \Lambda^{HE} & \Lambda^{HH} \end{pmatrix} \tag{11}$$

of resonators system within the unit cell of lattice. It takes into account both the intrinsic properties of isolated objects and their interactions with the environnement [18] (particles and interfaces). The dipspersion relations of resonant modes inside the system of coupled resonators is then given by the eigenvalues of the dress polarizability tensor.

Beside the spectrum of nanoresonators network we can calculate the amount of energy which is dissipated by the electromagnetic field inside each resonator. According to the Pynting's theorem [19] the power dissipated at a frequency ω inside the m^{th} resonator is given by the rate of doing work by the electric and mgnetic fields inside the resonator volume V_m

$$\mathscr{P}_m(\omega) = \frac{1}{2}\sum_{A=E,H}\int_{V_m} Re[\mathbf{j}_{m;A}^*(\mathbf{r},\omega).\mathbf{A}(\mathbf{r},\omega)]d\mathbf{r}. \tag{12}$$

Here $\mathbf{A}$ denotes either the local electric or magnetic field $\mathbf{E}$ and $\mathbf{H}$ while $\mathbf{j}_E$ and $\mathbf{j}_H$ are the corresponding local current density. In the dipolar approximation $\mathbf{j}_{m;A} = -i\omega\mathbf{p}_{m;A}\delta(\mathbf{r}-\mathbf{r}_i)$, expression (12) can be recasted into the discrete form

$$\mathscr{P}_m(\omega) = -\frac{\omega}{2}\sum_{A=E,H}\{Im[\mathbf{p}_{m;A}^*(\omega).\mathbf{A}_m^{ext}(\omega)] - \frac{\omega^3\mu_0}{2}\mathbf{p}_{m;A}^* Im[\mathbb{G}_0^{AA}(\mathbf{r}_m,\mathbf{r}_m)]\mathbf{p}_{m;A}\}. \tag{13}$$

By inverting (1) after having replaced the dipole moments by their expression with respect to $\mathbf{A}_m^{ext}$, we can express $\mathbf{A}_m^{ext}$ in term of $\mathbf{A}_{inc}$ and explicitely calculate the power dissipated in each object under an external lighting.

For spherical particles of radius R the polarizability is straightforwardly derived from the Mie scattering theory [20, 21]. If those particles, of refractive index n_m, are immersed inside a medium of index n_h, we have $\overleftrightarrow{\alpha}_A = \alpha_A\mathbb{1}$ with

$$\alpha_E{}^{-1} = k_0^3\frac{n_h}{6\pi}(C_E - i), \tag{14}$$

$$\alpha_H{}^{-1} = k_0^3\frac{n_h^3}{6\pi}(C_H - i). \tag{15}$$

Here k_0 is the wavevector inside vacuum and

$$C_E = \frac{\frac{\rho_m^2-\rho_h^2}{\rho_m^2\rho_h^2}(Cos\rho_h + \rho_h Sin\rho_h)(Sin\rho_m - \rho_m Cos\rho_m) + \rho_m Cos\rho_h Cos\rho_m + \rho_h Sin\rho_h Sin\rho_m}{\frac{\rho_h^2-\rho_m^2}{\rho_m^2\rho_h^2}(Sin\rho_h - \rho_h Cos\rho_h)(Sin\rho_m - \rho_m Cos\rho_m) - \rho_m Sin\rho_h Cos\rho_m + \rho_h Cos\rho_h Sin\rho_m}, \tag{16}$$

$$C_H = \frac{-\rho_h^2 Cos\rho_h(Sin\rho_m - \rho_m Cos\rho_m) + \rho_m^2 Sin\rho_m(Cos\rho_h + \rho_h Sin\rho_h)}{\rho_h^2 Sin\rho_h(Sin\rho_m - \rho_m Cos\rho_m) - \rho_m^2 Sin\rho_m(Sin\rho_h - \rho_h Cos\rho_h)} \tag{17}$$

with $\rho_h = k_0 n_h R$ and $\rho_m = k_0 n_m R$, n_m being the refractive index of resonator. According to Eqs. (13), (16) and (17) it follows that the power dissipated in each particle can be expressed both in

term of absorption cross-sections and of incident external field

$$\begin{aligned}\mathscr{P}_m(\omega) = -\frac{\omega}{2}\{&\varepsilon_0\frac{n_h\omega^3}{6\pi c^3}Im[\mathbf{E}_m^{ext*}(C_E\overleftrightarrow{\alpha}^*_{E,m}\overleftrightarrow{\alpha}_{E,m})\mathbf{E}_m^{ext}]\\ &+\mu_0\frac{n_h^3\omega^3}{6\pi c^3}Im[\mathbf{H}_m^{ext*}(C_H\overleftrightarrow{\alpha}^*_{H,m}\overleftrightarrow{\alpha}_{H,m})\mathbf{H}_m^{ext}]\}\end{aligned} \tag{18}$$

3. Generalization of scattering problem beyond the dipolar approximation

So far, we have only considered interactions between electric (resp. magnetic) dipoles. In this paragraph we describe how to take into account the multipolar interactions. The electromagntic field inside a medium of refractive index n_h can be expressed in term of ingoing (-) and outgoing (+) vector spherical wave functions (which form a complete basis)

$$\psi_{pq}^{\pm} = \begin{pmatrix} \mathbf{E}_{pq}^{\pm} \\ \mathbf{H}_{pq}^{\pm} \end{pmatrix} \tag{19}$$

where we have adopted the usual convention for the multipolar index (m,n) which are replaced by a single index $p = n(n+1)+m$ and where q set the polarization state (i.e. $q=1$ for TE waves and $q=2$ for TM waves).

The outgoing wave functions ψ_{pq}^{+} are solutions of Maxwell's equation (using the $e^{-i\omega t}$ convention)

$$\begin{cases}\nabla\times\mathbf{E}_{pq}^{+} = i\omega\mu\mathbf{H}_{pq}^{+}+\mathbf{H}_{pq}^{S}\\ \nabla\times\mathbf{H}_{pq}^{+} = -i\omega\varepsilon\mathbf{E}_{pq}^{+}+\mathbf{E}_{pq}^{S}\end{cases}. \tag{20}$$

with the source term $\psi_{pq}^{S} = \begin{pmatrix} \mathbf{E}_{pq}^{S} \\ \mathbf{H}_{pq}^{S} \end{pmatrix}$ (i.e. the multipole pq) defined by

$$\begin{cases}\mathbf{E}_{pq}^{S} = \mathbf{0}\\ \mathbf{H}_{pq}^{S} = in_h^{1/2}\mathbf{r}.D_n^m\end{cases}. \tag{21}$$

for the magnetic contributions and by

$$\begin{cases}\mathbf{E}_{pq}^{S} = -in_h^{-1/2}\mathbf{r}.D_n^m\\ \mathbf{H}_{pq}^{S} = \mathbf{0}\end{cases}. \tag{22}$$

for the electric ones where D_n^m expresses in term of partial derivative of the Dirac distribution δ as

$$\begin{aligned}D_n^m = &\frac{i}{(2k_0n_h)^n n!}\sqrt{\frac{8\pi(-1)^m(2n+1)(n-m)!}{n(n+1)(n+m)!}}\times\\ &\left\{z(\frac{\partial}{\partial x}+i\frac{\partial}{\partial y})-(x+iy)\frac{\partial}{\partial z}\right\}^{(n+m)}(-\frac{\partial}{\partial x}+i\frac{\partial}{\partial y})^{(n)}\delta.\end{aligned} \tag{23}$$

Let us consider an isolated particle of arbitrary shape immersed inside a host medium of index n_h and highlighetd by an external electromagnetic field. By definition, this field can be decomposed on the complete basis of $\psi_{pq}^{\pm}$ as

$$\mathbf{A}_{inc}(\mathbf{r}) = \sum_{pq}A_{inc}^{pq}\frac{\psi_{pq}^{+}(\mathbf{r})+\psi_{pq}^{-}(\mathbf{r})}{2}. \tag{24}$$

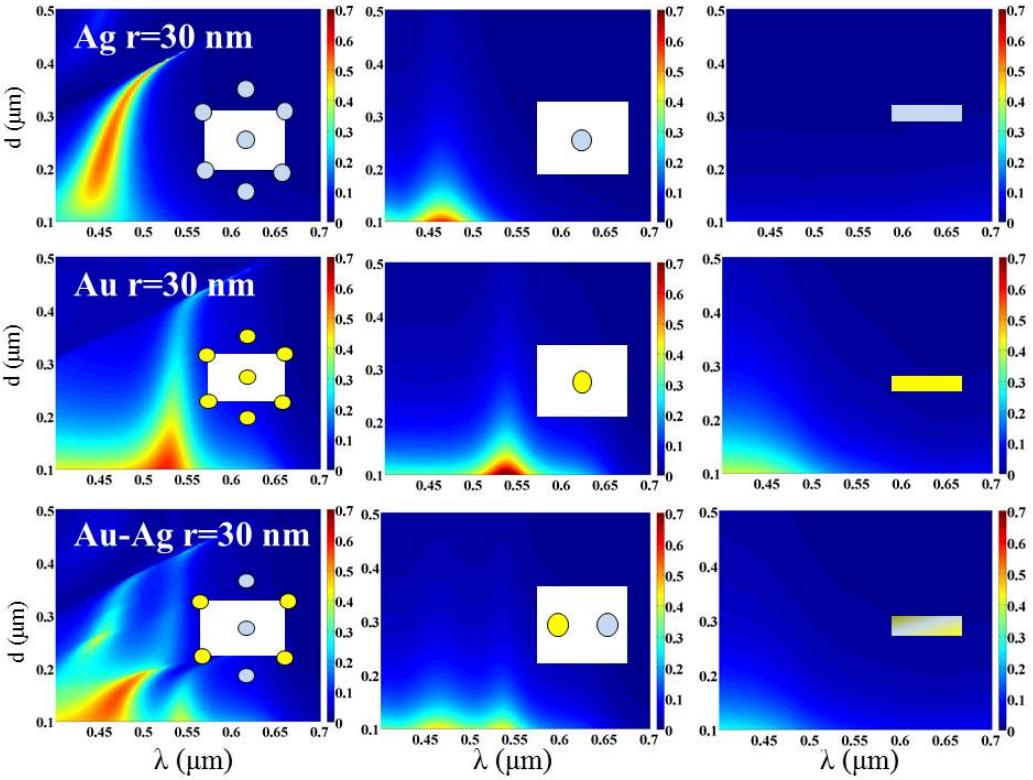

Fig. 2. On the first column, absorption of simple and binary hexagonal lattices made with Ag and Au nanoparticles 30 nm radius immersed at $h = 100nm$ from the surface in a transparent host medium of index $n_h = 1.5$ with respect to the density in particles. On the second column, this absoption is compared with the absorption of single particles without multiple scattering interaction and, on the last column, with the results given by the effective medium theory with the same filling factor.

As for the diffracted field, which is an outgoing field, it reads

$$\mathbf{A}_{diff}(\mathbf{r}) = \sum_{pq} A^{pq}_{diff} \psi^{+}_{pq}(\mathbf{r}). \tag{25}$$

To calculate the components A^{pq}_{diff} of the diffracted field we first calculate, by reciprocity and using the Lorentz relations [19] , the action of the sources $\psi^{S}_{p'q} = \begin{pmatrix} \mathbf{E}^{S}_{p'q} \\ \mathbf{H}^{S}_{p'q} \end{pmatrix}$ (with $p' = (n,-m)$) on the incident field. Then using the fact that $\psi^{\pm}_{pq}$ functions form a complete basis they satisfy the following orthogonality relations

$$\begin{cases} < \psi^{\pm}_{pq}, \psi^{\pm}_{p'q'} >= -4i\delta_{pq,p'q'} \\ < \psi^{\pm}_{pq} \psi^{\mp}_{p'q'} >= 0 \end{cases}. \tag{26}$$

where the brackets $< .,. >$ represents the scalar product in the Lorentz sens defined by

$$< \psi^{1}_{pq}, \psi^{2}_{pq} >= \oint (\mathbf{E}_1 \times \mathbf{H}_2 - \mathbf{E}_2 \times \mathbf{H}_1).\mathbf{n} dS. \tag{27}$$

Here, integration in taken over an oriented surface (with the vector $\mathbf{n}$) surrounding the particle. It follows by applying the Lorentz relation with the field $\psi^{+}_{p'q}$ generated by a source $\psi^{S}_{p'q}$ and the incident field $\mathbf{A}_{inc}$ that

$$< \psi^{+}_{p'q}, \mathbf{A}_{inc} >= \int \psi^{S}_{p'q}(\mathbf{r}).\mathbf{A}_{inc}(\mathbf{r})dr \equiv I_{\psi^{S}_{p'q}}[\mathbf{A}_{inc}]. \tag{28}$$

Note that $I_{\psi}[\mathbf{A}]$ is the action of the distribution on the test function ψ [22]. Then using the orthogonality relations (26) and according to (24)

$$A^{pq}_{inc} = \frac{i}{2} I_{\psi^{S}_{p'q}}[\mathbf{A}_{inc}]. \tag{29}$$

Then, using the matrix $\mathbf{T}$ which relates the vectors $\mathbf{A}_{inc}$ of components of incident field to the vector $\mathbf{A}_{diff}$ of diffracted field we have

$$A^{pq}_{diff} = \frac{i}{2} \sum_{pq} \mathbf{T}_{pq,p'q'} I_{\psi^{S}_{p'q}}[\mathbf{A}_{inc}], \tag{30}$$

Now, interactions between distinct particles dispersed inside a multilayer can be studied using a generalized form of the translation matrix as introduced by Stout et al. [23] to express the field generated by a source inside a particle in term of components of incident field on another particle.

4. Broadband absorber design

Now the general theoretical framework needed to describe the cooperative electromagnetic interaction inside a network of optical resonators we discuss in this paragraph how to use it to design targeted optical properties. To start with this objective ans show the strong potential of cooperative interactions we first consider the simple geometric configurations as illustrated in Fig. 2, that is single and binary metallic [24] particle arrays dispersed in regular hexagonal lattices of side length d and compare their absorption spectra with that ones of isolated particles and of homogeneous metallic film. All lattices are immersed in a transparent material of refractive index $n_h = 1.5$ and are maintained at a distance $h = 100nm$ from the surface. The results plotted in Fig. 2 clearly show that the resonance peaks in single particle lattices are essentialy centered at the resonance frequency of free particles. On the other hand the absorption spectrum of nanoparticles lattices is much broder and does not simply consist in a superposition of single particle spectra. Moreover, we see that the cooperative interactions allow increasing the absorption even in diluted lattices where the filling factor f is smaller than 3%. Finally, the comparison of the overall absorption of nanoparticle lattices with that of simple metallic films with a thickness defined, using the effective medium theory, from the nanoparticle filling factors points out the prime importance of cooperative effects to magnify the absorption level. In binary lattices, new configurationnal resonances add up to the resonances of single lattices and naturally enlarge the absorption spectrum.

In light of these results we can introduce a rational design of cooperative electromagnetic interactions to optimze the optical properties of a composite structure made with a distribution of nanoparticles. For this purpose we present the inverse design of a broadband absorber in the visible range [6, 25, 26, 27] made with a n-ary array metallic spherical nanoparticles. A n-ary lattice is defined from a unit cell $\mathscr{C}$ of a two dimensional paving with a certain thickness (see Fig. 3). In the unit cell of a lattice we consider a set of n vectors $\mathbf{r}_i$ and n positive reals R_i that represent the location of particles center and the radius of particles, respectively. To avoid the particle interpenetration these vectors must satisfy to the supplemental constraint $| \mathbf{r}_i - \mathbf{r}_j | > R_i + R_j$.

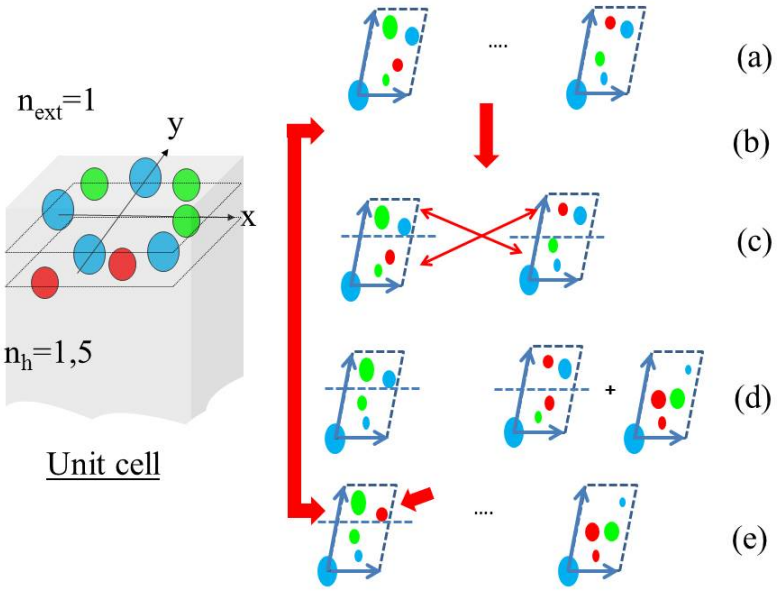

Fig. 3. Evolutionary algorithm to optimize a n-ary lattice. (a) A random population of periodic lattices (a physical view of an unit cell is plotted on the left) is randomly generated. (b) The best individus basd on the fitness function are selected as parents for the crossing over. (c) The next generation is created by linear crossing and completed by new individus (d) to keep the total population constant. (e) Mutations are aaplied on a few number of individus (typically 5%) in the current generation.

To design the n-ary lattice in order to maximize its overalll absorption we have to explore the large and complex space of all possible configurations. To do that we employ a genetic algorithm (GA) [28] which is a stochastic global optimisation method that is based on natural selection rules in a similar way to the Darwin's theory of evolution. Evolutionary optimization has been yet successfully applied in numerous fields of optics [29, 30].

Basically, a GA uses an initial population (Fig. 3) of typically few hundreds of structures also called individus which are randomly generated in size and position. For each individu we calculate the fitness parameter which is here the mean absorption (for a given polarization) $\overline{A} = (\lambda_{max} - \lambda_{min})^{-1} \int_{\lambda_{min}}^{\lambda_{max}} A(\lambda) d\lambda$ over the spectral range $[\lambda_{min}; \lambda_{max}]$ where we want to increase the absorption. The monochromatic absorption $A(\lambda)$ at a given wavelength is simply given by the the sum of power dissipated inside the particles of the unit cell normalized by the incident flux $\phi_{inc}(\lambda)$ on its surface $\mathscr{S}$ that is

$$A(\lambda) = \frac{\sum\limits_{m \in Cell} \mathscr{P}_m(\lambda)}{\mathscr{S} \phi_{inc}(\lambda)}. \tag{31}$$

The GA consists in maximizing the fitness function of structures (i.e. $\overline{A} \rightarrow max$). To do so, we select 90% of the highest fitness as future parents for the next generation of selecting process. Those parents are linear crossed and the new 'child' generation is completed by new individual structures (randomly generated) to keep the same total number of lattices for any generation. To

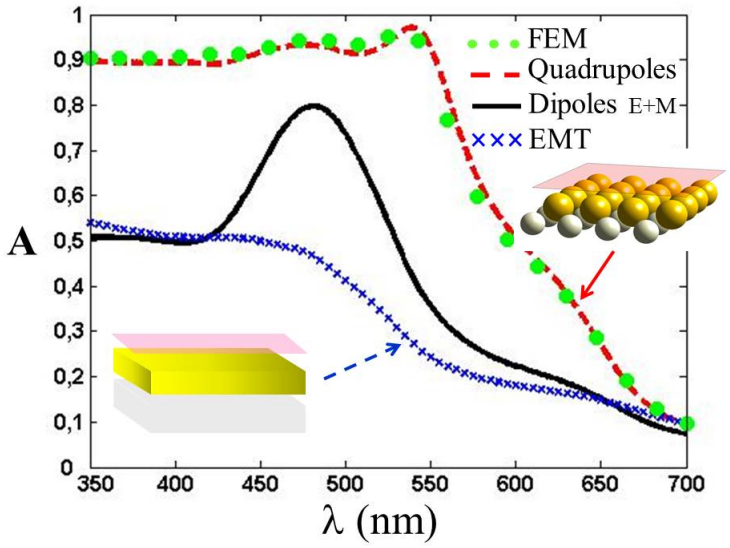

Fig. 4. Light absorption spectrum at normal incidence of a binary Au-Ag lattice (red dashed curve) optimized by GA by taking into account all multipolar interactions until the second order (quadrupoles) and of a multilayer based on Au-Ag films of thickness defined with the filling factor in nanoparticles (i.e. effective medium theory). Circles curve shows the result obtained by solving the Maxwell's equations with a finite element method.

avoid the convergence toward local extrema, every m (typically 10) generations, we introduce also some mutations that is to say random perturbations with a probability of about 5% on the value of parameters we are optimizing. The results presented in Fig. 4 for superposed binary Au-Ag lattices (with the radius $r_{Au} = 77nm$ and $r_{Ag} = 39nm$, the separation distances from the surface $h_{Au} = 120nm$ and $h_{Ag} = 242nm$, the lattice constants $d_{Au} = d_{Ag} = 200nm$ and the off-centring $e_x = 56nm$ and $e_y = 10nm$) exhibit a broad absorption band in the visible range. By taking into account the multipolar interactions until the second order (i.e. quadrupolar interactions) we see that the level of aborption becomes close to one. The comparaison of these results with full electromagnetic simulations based on the finite element method shows that the higher order multipole moments do not contribute significantly to the overall absorption. The absorption enhancement can be understood by examinating the electromagnetic cooperative effects inside the structure. These effects are highlighted in Fig. 5 at two different wavelengths by plotting the local losses inside the gold (resp. silver) nanoparticles within the optimized binary lattice in presence or without silver (resp. gold) nanoparticles. At $\lambda = 550nm$, that is to say, at the resonance of gold particles (which corresponds to the region where we observe in Fig. 4 an important bump in the absorption spectrum when it is calculated in the dipolar approximation) we see that the presence of silver nanoparticles enhance by 20% the losses inside the gold particles. Similarly, at $\lambda = 650nm$, the gold particles enhance by a factor of 60% the dissipation inside the silver particles. However, because of the weakness of intrinsic losses inside isolated Ag particles this cooperative effect is not sufficiently important to increase the overall absorption of the structure. At low wavelength we have checked (not plotted in Fig. 5) that the high absorption levels as shown in Fig. 4 results from cooperative effects between the gold particles themselves. The silver particles do not play any role in the exaltation mechanism.

Interestingly, the numerical simulations have shown also that the cooperative effects are not

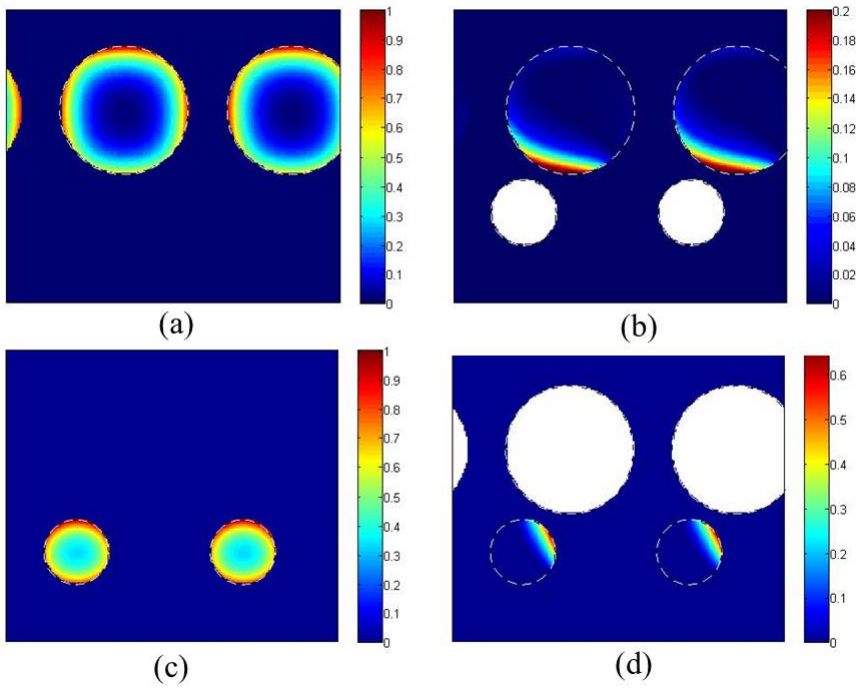

Fig. 5. Local losses at $\lambda = 550nm$ in the particles of a gold nanoparticle lattice (a) with the same geometric parameters as in the optimized structure. Losses $\Im(\varepsilon)|E_{SG}|^2$ in the single particle lattice are normalized by the maximum loss. In (b) we show the normalized difference $\Im(\varepsilon)|E_{DG}|^2 - \Im(\varepsilon)|E_{SG}|^2$ of losses inside Au particles in presence and without Ag particles (white regions). Analogously, in (c) and (d) the cooperative effect induces by the presence of Au particles on the dissipation in the Ag particles is shown at $\lambda = 650nm$.

very sensitive to the presence of disorder. In Fig. 6 we show, by disturbing the optimal structure with a -random perturbation of particles locations by a maximum displacement of $20nm$, that the discrepancy between the optimal structure and the perturbed ones, given by the mean square error $\zeta = [\int_{\lambda_{min}}^{\lambda_{max}} (A(\lambda) - A_{opt}(\lambda))^2 d\lambda]^{1/2}$, remains small. For some realization a broadening of spectrum can be observed around 650 nm. This effect can attributed to the presence of new modes supported which give rise to new channels for dissipating light energy within the structure. However, the detailed study of random structures goes far beyond the scope of the present work and it will be carried out in a future work.

5. Conclusion

In conclusion, we have proposed a general method for engineering the cooperative electromagnetic interactions in resonators networks both in the dipolar approximation and for arbitrary multipolar orders. Our results have demonstrated the strong potential of these interactions to tailor the optical properties spectrum. We believe that this approach opens the way to a rational design of metamaterials and it could find broad applications in various fields of applied physics, as for instance, in the domain of photovoltaic energy conversion for the conception of more efficient solar cells, in optical information treatement for the design of quantum information systems and, according to the reciprocity principle [31], in light extraction technologies to

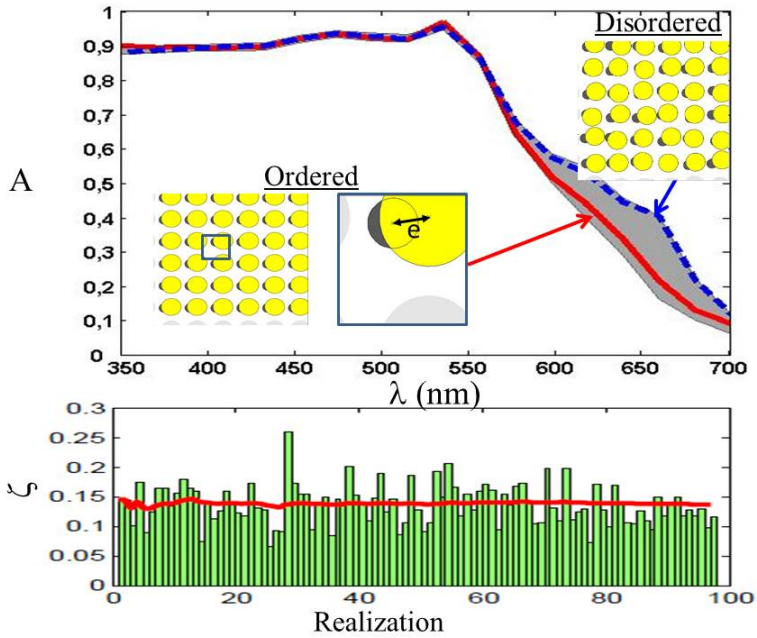

Fig. 6. Impact of disorder on the light absorption spectrum at normal incidence in a binary Au-Ag lattice.The spatial location of particles is randomly perturbated by a displacement of 20*nm*. The red ciurve corresponds to the spectrum (in polarization TM at nomrla incidence) of the optimized structure and the dotted blue curve is the spectrum of a particular random realization (results in polarization TE, not plotted here are similar). The dashed area shows the maximum and minimm values of absorption spectrum of different random realizations. The histogram shows the discrepancy with the optimal fintess for different realizations of the structure. The red line on the histogram shows the mean error with respect to the number of realizations.The disorder is mimicked by using pseudoperiodic particle array with sufficiently large unit cells.

improve the performances of light emitting diodes.

Acknowledgments

J.-P. H. acknowledges discussions with J.J. Greffet. P. B.-A. gratefully acknowledges the support of Total news energies.